Borehole guided waves in a non-Newtonian (Maxwell) fluid-saturated porous medium*

Cui Zhi-Wen(崔志文)[a)†], Liu Jin-Xia(刘金霞)[a)],
Yao Gui-Jin(姚桂锦)[b)], and Wang Ke-Xie(王克协)[a)]

[a)] *Department of Acoustics and Microwave Physics, School of Physics, Jilin University, Changchun* 130021, *China*
[b)] *The School of Communication Engineering, Jilin University, Changchun* 130012, *China*

(Received 1 January 2010; revised manuscript received 22 January 2010)

The property of acoustic guided waves generated in a fluid-filled borehole surrounded by a non-Newtonian (Maxwell) fluid-saturated porous formation with a permeable wall is investigated. The influence of non-Newtonian effects on acoustic guided waves such as Stoneley waves, pseudo-Rayleigh waves, flexural waves, and screw waves propagations in a fluid-filled borehole is demonstrated based on the generalized Biot–Tsiklauri model by calculating their velocity dispersion and attenuation coefficients. The corresponding acoustic waveforms illustrate their properties in time domain. The results are also compared with those based on generalized Biot's theory. The results show that the influence of non-Newtonian effect on acoustic guided wave, especially on the attenuation coefficient of guided wave propagation in borehole is noticeable.

Keywords: borehole, guided waves, Maxwell fluid, porous medium

PACC: 4320, 9130, 0350D

1. Introduction

The acoustical properties of porous materials can generally be described in a wide frequency range with Biot's theory,[1] which involves the determination of a number of physical parameters. The theory of the elastic wave propagation in the fluid-saturated porous medium was first developed by Biot directly at a macroscopic level. Biot (1956), in his derivation of wave propagation in porous medium, treated the viscous pore fluid as Newtonian fluid. Biot's acoustic wave theory is a general and powerful technique for understanding the composite elastic properties of fluid-saturated porous medium. Biot's theory has been a successful tool for interpreting experiment data for decades, and has been applied in fields as diverse as geophysics and bone.[2−5] Hydrocarbon exploration is especially concerned with porous formation. In acoustic logging, the guided waves that propagate along the borehole are affected by the properties of the formation.[6] The amplitude and the travel-time characteristics of guided waves in a fluid-filled borehole carry important information about properties of surrounding formation. The information about the guided waves is very important for determining the parameter of formation. In order to interpret logging data properly, one needs a thorough understanding of the propagations of different elastic guided waves in a fluid-filled borehole.

Many authors have studied the properties of elastic waves propagation in the fluid borehole by using Biot's theory on the assumption that the permeable formation around the fluid borehole is Newtonian fluid-saturated porous medium.[7−13] But for oil and other hydrocarbons, which often exhibit significant non-Newtonian behaviours,[14] Biot model is not applicable any more. Recently, Tsiklauri and Beresnev[15] introduced non-Newtonian effect into the classic Biot theory, treated the pore fluid as non-Newtonian (Maxwell) fluid and studied the properties of elastic wave propagation in such a fluid-saturated porous medium.[16] Their work provides a more complete theory of the flow of Maxwell fluid through a longitudinally oscillating cylindrical tube with an oscillating pressure gradient, which has important practical applications. Cui *et al.*[17] derived the mathemat-

*Project supported by the National Natural Science Foundation of China (Grant Nos. 40974067, 40674059 and 10534040) and the State Key Laboratory of Acoustics, Chinese Academy of Sciences (Grant No. 200807), and Scientific Forefront and Interdisciplinary Innovation Project of Jilin University (Grant No. 200903319).
†Corresponding author. E-mail: cuizw@jlu.edu.cn
© 2010 Chinese Physical Society and IOP Publishing Ltd

ical expressions of viscosity correction factor $F_m(\omega)$ for a Maxwell fluid-saturated porous medium with an arbitrary pore size distribution and investigated the elastic waves in such a medium. The studies[16−18] have shown that the non-Newtonian effect of pore fluid plays an important role in wave propagation in a saturated medium because it leads to wave dispersion and is responsible for the dissipation of energy in propagation.

The purpose of this paper is to investigate the influence of non-Newtonian effect on guided wave propagation in a fluid-filled borehole. In the present work, based on the generalized Biot–Tsiklauri model[17] with a no-slip boundary, we pay attention to the influence of non-Newtonian effect on velocity and attenuation coefficients of the fundamental guided waves excited by a monopole, a dipole and a quadrupole source. The acoustic guided waveforms using the discrete wavenumber method and the curves of velocity dispersion and attenuation coefficients of the fundamental guided waves are investigated.

2. Theoretical basis

2.1. Generalized Biot–Tsiklauri model

In Biot's theory, a fluid-saturated porous medium is regarded as an interacting two-phase elastic system, of which one phase is a porous solid skeleton and the other phase is a fluid filling the voids. We describe the viscoelastic effect of the fluid filling the voids by using Maxwell's model, which assumes that

$$t_{\mathrm{m}}\partial\boldsymbol{\tau}_{\mathrm{v}}/\partial t = -\eta\nabla\boldsymbol{v} - \boldsymbol{\tau}_{\mathrm{v}}, \tag{1}$$

where η is the viscosity coefficient, t_{m} is the relaxation time (hereafter m denotes Maxwell) and $\boldsymbol{v}$ denotes the velocity of the fluid, whereas $\boldsymbol{\tau}_{\mathrm{v}}$ represents the viscous stress tensor. Here, we use D_{e} to denote the Deborah number, which is defined as the ratio of characteristic time viscous effect ($t_{\mathrm{v}} = \rho_{\mathrm{f}}a_{\mu}^2/\eta$, a_{μ} is the radius of pore) to relaxation time, i.e., $D_{\mathrm{e}} = t_{\mathrm{v}}/t_{\mathrm{m}}$. It is the Deborah number that determines in which regime the system resides. For a small value of D_{e}, the system exhibits a viscoelastic behaviour, which we call the non-Newtonian regime. The equations of motion in the porous medium are[17]

$$\begin{aligned} &G\nabla^2\boldsymbol{u} + (H-G)\,\nabla\nabla\cdot\boldsymbol{u} + C\nabla\cdot\boldsymbol{w} \\ &= \frac{\partial^2}{\partial t^2}\left(\rho\boldsymbol{u} + \rho_{\mathrm{f}}\boldsymbol{w}\right), \end{aligned} \tag{2}$$

$$\nabla\left(C\nabla\cdot\boldsymbol{u} + M\nabla\cdot\boldsymbol{w}\right) = \frac{\partial^2}{\partial t^2}\left(\rho_{\mathrm{f}}\boldsymbol{u} + \rho_{\mathrm{m}}\boldsymbol{w}\right), \tag{3}$$

where H, C and M are the generalized elastic coefficients deduced by Biot and expressed as

$$\begin{aligned} H &= K_{\mathrm{b}} + 4G/3 + (1 - K_{\mathrm{f}}/K_{\mathrm{s}})C, \\ C &= (1 - K_{\mathrm{f}}/K_{\mathrm{s}})M, \\ M &= K_{\mathrm{f}}K_{\mathrm{s}}/\left[\phi K_{\mathrm{s}} + (1 - K_{\mathrm{f}}/K_{\mathrm{s}} - \phi)\,K_{\mathrm{f}}\right], \end{aligned} \tag{4}$$

where K_{s}, K_{f}, K_{b} and G denote the solid grain modulus, the pore fluid bulk modulus, the framework modulus, and the shear modulus. These quantities are measurable for a porous medium. The $\boldsymbol{w} = \phi\left(\boldsymbol{u}_{\mathrm{f}} - \boldsymbol{u}\right)$ represents the flow of the fluid relative to solid and is measured in the terms of volume per unit area of the bulk medium, where $\boldsymbol{u}_{\mathrm{f}}$ and $\boldsymbol{u}$ are the absolute displacements of the pore fluid phase and the solid phase of a porous medium, respectively, and ϕ is a total porosity. The density of bulk can be expressed by grain density ρ_{s} and pore fluid density ρ_{f} as $\rho = (1-\phi)\,\rho_{\mathrm{s}} + \phi\rho_{\mathrm{f}}$. The effective density of the fluid in relative motion is $\rho_{\mathrm{m}} = \mathrm{i}\,\eta/\omega\kappa(\omega)$. Biot's dynamic permeability $\kappa(\omega)$ can be expressed as

$$\kappa(\omega) = \kappa_0[F_{\mathrm{m}}(\omega) - \mathrm{i}\,\omega/\omega_{\mathrm{c}}]^{-1}. \tag{5}$$

Here $\kappa(\omega)$ describes the response of the fluid-saturated porous medium to an applied stimulus, and characterizes the frequency-dependent behaviour of pore fluid flow. The $F_{\mathrm{m}}(\omega)$ is the viscosity correction factor which is generalized to the case of a non-Newtonian (Maxwell) fluid with an arbitrary pore size distribution.[17] It measures the deviation from Poiseuille flow friction as a function of frequency, i.e.

$$F_{\mathrm{m}}(\omega) = \mathrm{i}\,\frac{\omega}{\omega_{\mathrm{c}}}\frac{Z(\omega)}{Z(\omega)-1}, \tag{6}$$

where

$$Z(\omega) = \int_0^{\infty}\frac{2\mathrm{J}_1(\beta a)}{\beta a\mathrm{J}_0(\beta a)}f(a)\mathrm{d}a,$$

$\beta^2 = (\omega^2 t_{\mathrm{m}} + \mathrm{i}\,\omega)\rho_{\mathrm{f}}/\eta$, $\mathrm{J}_0(x)$ and $\mathrm{J}_1(x)$ are Bessel functions of orders 0 and 1, $\omega_{\mathrm{c}} = \phi\eta/\rho_{\mathrm{f}}\kappa_0$ is Biot's transition frequency, κ_0 is the effective permeability of porous medium, which can be obtained from $\kappa_0 = \int_0^{\infty}(\phi/8)a^2 f(a)\mathrm{d}a$, with a being pore radius, and $f(a)$ being a radial probability density distribution function.

2.2. Solutions for borehole guided waves

We adopt the cylindrical coordinate system (r, θ z) with the z axis along the borehole axis. The model consists of a fluid-filled borehole of radius R, extending to infinity in the z direction, embedded in a

radically semi-infinite isotropic porous formation saturated by a non-Newtonian (Maxwell) fluid. The fluid contained in the borehole is assumed to be inviscid and ideally compressible, i.e., it cannot support shear stresses making the state of stress in the fluid purely hydrostatic. We consider multipole sources described by Kurkjian and Chang.[19] The compressional waves that are trapped in the inviscid fluid layer inside the borehole may be expressed as

$$\varphi_n^{\mathrm{f}} = \zeta_0 \left[\varepsilon_n \mathrm{K}_n(\nu r) + A\mathrm{I}_n(\nu r)\right] \cos n(\theta - \theta_0), \quad (7)$$

where $\zeta_0 = (\nu r_0/2)^n/n!$, r_0 and θ_0 are the distribution radius and the azimuthal angle of multipole source, respectively, θ is the azimuthal angle of field point, I_n and K_n are the n-th-order modified Bessel functions of first kind and second kind, respectively, n denotes the type of multipole source ($n = 0$, $\varepsilon_n = 1$; $n \neq 1$, $\varepsilon_n = 2$), $\nu^2 = k_z^2 - \omega^2/V_{\mathrm{f}}^2$ is the radial wavenumber of fluid, k_z is the axial wavenumber, A is the weighting coefficient, $u_n^{\mathrm{f}} = \partial\varphi_n^{\mathrm{f}}/\partial r$ and $P_n^{\mathrm{f}} = \omega^2\rho_{\mathrm{f}}\varphi_n^{\mathrm{f}}$ are radial displacement and pressure of the fluid inside borehole respectively.

The medium outside the borehole is a two-phase medium described by Biot–Tsiklauri model. Introduce the displacement potentials in the convenient fashion as follows:

$$\boldsymbol{u} = \nabla\varphi_{\mathrm{p1}} + \nabla\varphi_{\mathrm{p2}} + \nabla\times(\chi\boldsymbol{e}_z) + \nabla\times\nabla\times(\psi\boldsymbol{e}_z), \quad (8)$$

$$\boldsymbol{w} = \nabla\alpha_{\mathrm{p1}}\varphi_{\mathrm{p1}} + \nabla\alpha_{\mathrm{p2}}\varphi_{\mathrm{p2}} + \nabla\times(\alpha_{\mathrm{s}}\chi\boldsymbol{e}_z) + \nabla\times\nabla\times(\alpha_{\mathrm{s}}\psi\boldsymbol{e}_z), \quad (9)$$

where φ_{p1} and φ_{p2} are compressional potentials of fast compressional wave and slow compressional wave, χ is horizontal polarized shear potential (SH wave) and ψ is vertical polarized shear potential (SV wave), the expressions of α_ξ (ξ=p1, p2, s) are similar to those in Refs. [20] and [21]. Because the radiation conditions prescribe that the displacement potential of formation keeps finite when r tends to infinity, the particular solutions in the frequency-axial wavenumber with respect to an n-th-order mutipole, are

$$\begin{aligned}
\varphi_{\mathrm{p1}} &= \zeta_0 B\mathrm{K}_n(\nu_{\mathrm{p1}} r)\cos n(\theta-\theta_0),\\
\varphi_{\mathrm{p2}} &= \zeta_0 C\mathrm{K}_n(\nu_{\mathrm{p2}} r)\cos n(\theta-\theta_0),\\
\psi_{\mathrm{s}} &= \zeta_0 D\mathrm{K}_n(\nu_{\mathrm{s}} r)\cos n(\theta-\theta_0),\\
\chi_{\mathrm{s}} &= \zeta_0 E\mathrm{K}_n(\nu_{\mathrm{s}} r)\sin n(\theta-\theta_0),
\end{aligned} \quad (10)$$

$\nu_\xi^2 = k_z^2 - \omega^2 s_\xi^2$ (ξ=p1, p2), and $\nu_{\mathrm{s}}^2 = k_z^2 - \omega^2 s_{\mathrm{s}}^2$ are the radial wavenumbers relative to the compressional wave and the shear wave, s_ξ is the compressional wave slowness, s_{s} is the shear wave slowness,[20] and B, C, D and E are the weighting coefficients each as a function of axial wavenumber k_z and angular frequency ω. We can obtain the components of the displacement and the stress field in terms of the above potentials by Eq. (10) and the following equations:

$$\boldsymbol{\tau} = (H-2G)(\nabla\cdot\boldsymbol{u})\boldsymbol{I} + C(\nabla\cdot\boldsymbol{w})\boldsymbol{I} + G(\nabla\boldsymbol{u} + \nabla\boldsymbol{u}^{\mathrm{T}}), \quad (11)$$

$$-P = C\nabla\cdot\boldsymbol{u} + M\nabla\cdot\boldsymbol{w}. \quad (12)$$

A permeable interface is considered in this paper, and the boundary conditions at the borehole wall (i.e. at $r = R$) are:

$$\begin{aligned}
&u_r^{\mathrm{I}} = u_r^{\mathrm{II}} + w_r^{\mathrm{II}}; \quad -P_{\mathrm{f}}^{\mathrm{I}} = \tau_{rr}^{\mathrm{II}};\\
&P_{\mathrm{f}}^{\mathrm{I}} = P_{\mathrm{f}}^{\mathrm{II}}; \quad 0 = \tau_{rz}^{\mathrm{II}}; \quad 0 = \tau_{r\theta}^{\mathrm{II}}.
\end{aligned} \quad (13)$$

Here, superscripts I and II represent the media inside and outside the borehole, respectively. It is obtained that

$$\begin{pmatrix}
m_{11} & m_{12} & m_{13} & m_{14} & m_{15}\\
m_{21} & m_{22} & m_{23} & m_{24} & m_{25}\\
m_{31} & m_{32} & m_{33} & 0 & 0\\
0 & m_{42} & m_{43} & m_{44} & m_{45}\\
0 & m_{52} & m_{53} & m_{54} & m_{55}
\end{pmatrix}
\begin{pmatrix} A\\ B\\ C\\ D\\ E \end{pmatrix} =
\begin{pmatrix} b_1\\ b_2\\ b_3\\ 0\\ 0 \end{pmatrix}, \quad (14)$$

where m_{ij} $(i, j \leq 5)$, b_1, b_2 and b_3 are similar to those in Ref. [12]. Because non-axismmetric wave cannot be excited by the monopole, the coefficient matrix in Eq. (14) is a 4×4 matrix when $n = 0$. The reflection coefficient can be written as $A(k_z,\omega) = N_n(k_z,\omega)/D_n(k_z,\omega)$, where $N_n(k_z,\omega)$ and $D_n(k_z,\omega)$ are the numerator and the denominator of the reflection coefficients, respectively. The poles corresponding to the guided waves can be determined by

$$D_n(k_z,\omega) = 0 \quad (n = 0, 1, 2, \ldots). \quad (15)$$

This is the dispersion equation of the guided waves. For a certain frequency, it gives the axis-wavenumber of guided wave propagation along the direction of the axis of the borehole, its root is corresponding to the pole k_l $(l = 1, 2, \ldots)$ of the reflection coefficient. It is assumed that the receivers are placed at the borehole axis to sense the pressure, the displacement and the spatial derivative of displacement when the source is a monopole, a dipole or a quadrupole, respectively. So the amplitude of the guided wave excited by a source is given by

$$a_n(k_l,\omega) = \frac{\mathrm{i}}{n!}\left(\frac{v^2 r_0}{4}\right)^n$$

$$\times \mathrm{e}^{\mathrm{i}\,k_z z} \frac{N_n\left(k_z,\omega\right)}{\partial D_n\left(k_z,\omega\right)/\partial k_z}\bigg|_{k_z=k_l}, \quad (16)$$

and the curves of guided waveforms can be expressed

$$g_n\left(z,t\right) = \frac{1}{2\pi}\int_{-\infty}^{\infty} V\left(\omega\right) a_n\left(k_l,\omega\right) \exp\left(-\,\mathrm{i}\,\omega t\right) \mathrm{d}\omega, \quad (17)$$

where $V\left(\omega\right)$ denotes the source spectrum. Any pole corresponds at a given frequency to a complex wavenumber root $k_l = \mathrm{Re}\left(k_l\right) + \mathrm{i}\,\mathrm{Im}\left(k_l\right)$ of the dispersion equation. The phase velocity of the mode is equal to $\omega/\mathrm{Re}\left(k_l\right)$, while its attenuation is equal to $2\,\mathrm{Im}\left(k_l\right)/\mathrm{Re}\left(k_l\right)$, then the group velocity is obtained by numerical differentiation from $\partial\omega/\partial\,\mathrm{Re}\left(k_l\right)$.

3. Numerical examples

In the following, we calculate the acoustic waveform and the curves of velocity dispersion, and attenuation coefficients of the fundamental guided wave due to a monopole, a dipole and a quadrupole source. The pore size a is given in μm and is related to γ by $\gamma = \ln a$. The pore radius probability density distribution function is

$$f\left(\gamma\right) = \frac{1}{\sqrt{2\pi}\sigma} \exp\left[-\frac{\left(\gamma-\bar{\gamma}\right)^2}{2\sigma^2}\right], \quad (18)$$

where $\bar{\gamma} = \ln a_\mu$ and σ^2 are the mean and the variance of log-transformed pore radius ($\ln a$) respectively, with a_μ being the median pore radius. The distribution of γ-normal standard is similar to that in Ref. [22].

We select the same parameters as those in Ref. [20], i.e. $K_\mathrm{f} = 2.25$ GPa, $K_\mathrm{s} = 38$ GPa, $K_\mathrm{b} = 16$ GPa, $G = 14.61$ GPa, $\rho_\mathrm{f} = 1000$ kg/m^3, $\rho_\mathrm{s} = 2650$ kg/m^3, $\phi = 0.1$, and $\eta = 0.001$ Pa·s. As in Ref. [22], we can obtain the permeability by $k_0 = \phi a_\mu^2 \mathrm{e}^{\left(2\sigma^2\right)}/8$. The $\sigma = 0$ corresponds to the case where all pore radii have the same sizes. The $\sigma \neq 0$ corresponds to the distribution of γ-normal standard. In this paper we choose $a_\mu = 6.3\times10^{-6}$ m and $\sigma = 0.7$. When $D_\mathrm{e} = \infty$ ($t_\mathrm{m} = 0$), this study corresponds to the generalized Biot theory with a pore size distribution developed by Yamamoto and Turgut.[17] Whatever the example is, the multipole separation (i.e., r_0) is 0.01 m, and synthetic waveforms in the time domain are shown at $z = 3$ m.

Figure 1 gives the phase velocities, the group velocities and the attenuations of the two types of modes excited by a monopole (axisymmetric) for three cases: the solid curve corresponds to $D_\mathrm{e} = \infty$, i.e. the Newtonian fluid-saturated case with pore size distribution, the dash and the dash-dot curves represent the non-Newtonian cases $D_\mathrm{e} = 10$ and $D_\mathrm{e} = 1$, respectively. The first axisymmetric mode is Stoneley wave. The Stoneley wave exists at all frequencies. This wave exhibits a slight dispersion and its energy is usually highest at low frequencies. The second axisymmetric mode is the pseudo-Rayleigh mode (in Fig. 1, we only show the fundamental modes, the higher modes are not plotted there), which has in this case a cut-off frequency. At this cut-off frequency, the mode reaches its highest phase velocity, namely the shear wave velocity of the formation. As the frequency of the waves increases, the phase velocity of the mode approaches the fluid velocity asymptotically from above. As the value of D_e decreases, only in the deeply non-Newtonian regime, the values of phase velocity and group velocity of the two types of guide waves have a little change. Namely, the influence of non-Newtonian effects on the velocities of the two types of guided waves is small. The results in Fig. 1(b) indicate that the influence of non-Newtonian effect is not significant on attenuation in the low frequency logging for Stoneley wave (blow 2 kHz). However, the attenuation of the Stoneley wave has an overall increase in an intermediate frequency range, especially in the deeply non-Newtonian regime. The attenuations of pseudo-Rayleigh modes in the deeply non-Newtonian regime are obviously much higher than those predicted by Biot's model. This means that the non-Newtonian effects on attenuations of the two types of guided waves are prominent.

Figure 2 shows the dispersions and the attenuations of the flexural mode excited by a dipole source for three cases as Fig. 1. The flexural waves (flex in short) are associated with a pure bending of the borehole. We also find that the dispersion curves of flexural mode have a little change only in the deeply non-Newtonian regime. Flexural waves are often used to obtain shear velocity, and the results show that formation fluid viscosity does not have a significant influence on velocity measurement. However, the attenuations in the deeply non-Newtonian regime are much higher than those in the Newtonian fluid-saturated case in an intermediate frequency range, to which we should pay attention even in the general non-Newtonian regime ($D_\mathrm{e} = 10$).

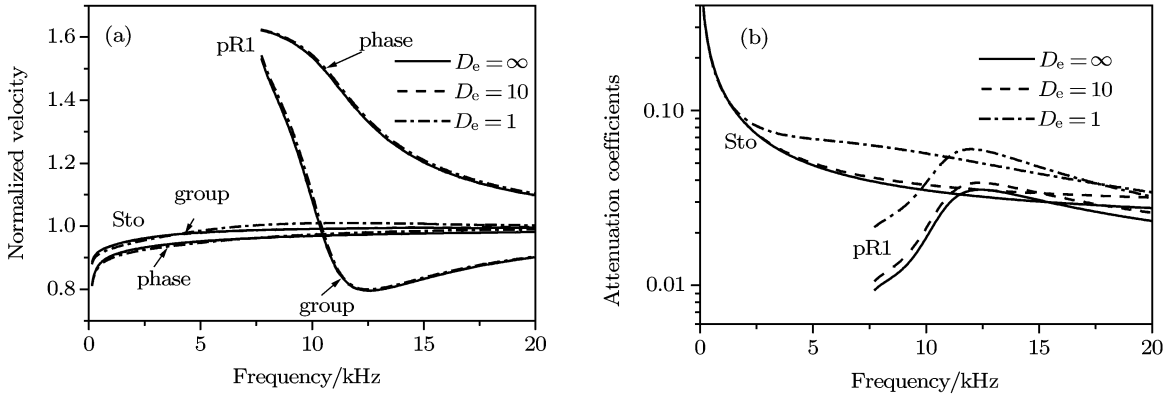


Fig. 1. Curves for dispersion (a) and attenuation coefficients (b) of guided waves excited by monopole source versus frequency, where velocity is normalized by velocity of borehole fluid.

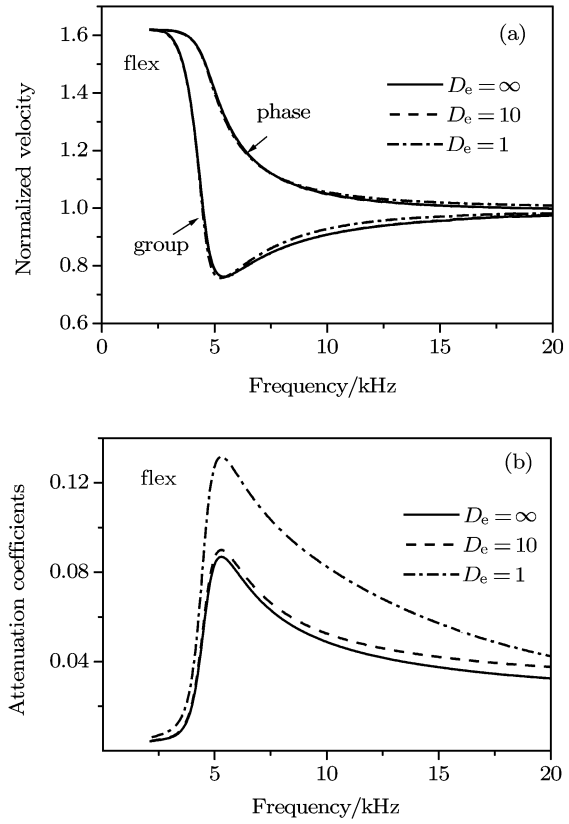


Fig. 2. Curves for dispersion (a) and attenuation coefficients (b) of guided waves excited by dipole source versus frequency, where velocity is normalized by velocity of borehole fluid.

Figure 3 shows the dispersions and the attenuations of the screw mode excited by a quadrupole source for three cases as Fig. 1. From Fig. 3 we can find that the dispersion and the attenuation of the screw mode are analogous to those of the flexural mode except for a shift toward higher frequencies. We also find that the dispersion curves of screw mode have a little change only in the deeply non-Newtonian regime. However, the attenuations in the deeply non-Newtonian regime are much higher than those in the Newtonian fluid-saturated case at intermediate frequencies, to which we should also pay attention even in the general non-Newtonian regime ($D_e = 10$). These results show that the non-Newtonian effect on attenuation of guided wave is noticeable.

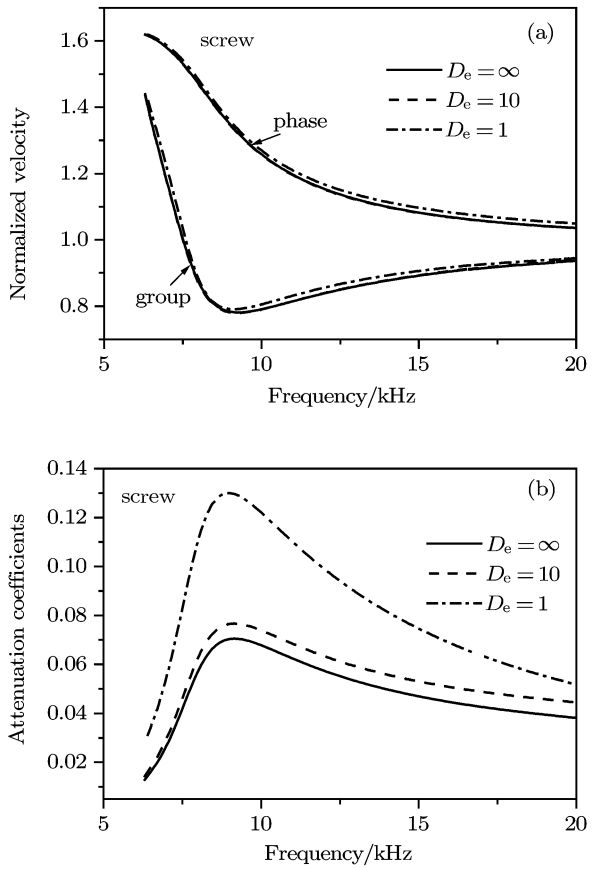


Fig. 3. Curves for dispersion (a) and attenuation coefficients (b) of guided waves excited by quadrupole source, where velocity is normalized by velocity of borehole fluid.

Figure 4(a) shows the waveforms of the Stoneley waves with 6-kHz source central frequency for three cases: dot curves correspond to the Newtonian limit when $D_e = \infty$, while thin and thick solid curves represent the non-Newtonian cases $D_e = 10$ and $D_e = 1$, respectively. In Fig. 4(a) we find that the arrival times of Stoneley waves are nearly the same as those based on the non-Newtonian fluid-saturated case and the Newtonian fluid-saturated case. However, as the value of D_e decreases, the amplitude of Stoneley wave becomes small, especially in the deeply non-Newtonian regime. Figure 4(b) shows the waveforms of the pseudo-Rayleigh wave with 10-kHz source central frequency for the three cases as Fig. 4(a). We also find that arrival times of pseudo-Rayleigh wave are almost unchanged. But the amplitude of the pseudo-Rayleigh wave in the deeply non-Newtonian fluid-saturated case is much smaller than that in the Newtonian fluid-saturated case, which becomes small even in the general non-Newtonian regime ($D_e = 10$). These are consistent with the dispersion and the attenuation curves in Fig. 1.

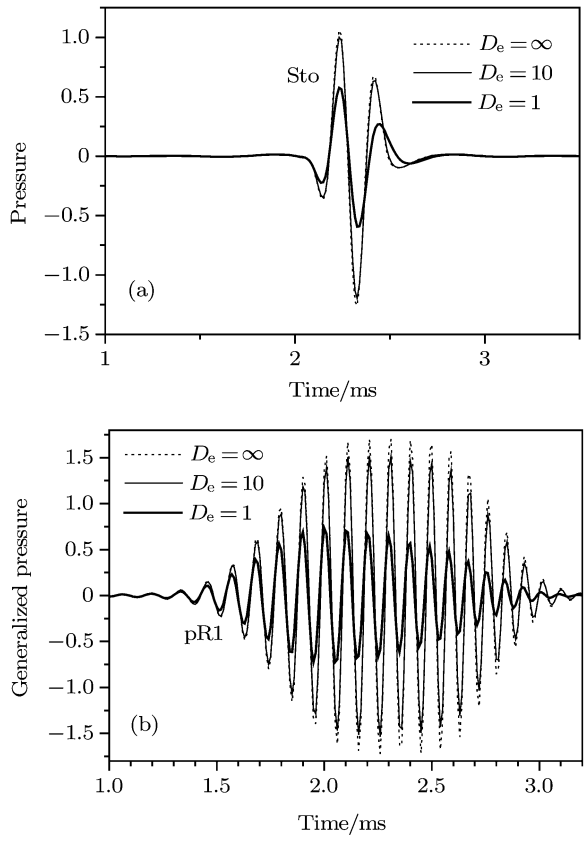


Fig. 4. Guided waveforms excited by monopole source. (a) Stoneley waves with 6-kHz source central frequency. (b) Pseudo-Rayleigh waves with 10-kHz source central frequency.

Figure 5 shows the waveforms of the flexural mode with 4-kHz source central frequency for three cases as Fig. 4. The arrival times of flexural mode are nearly the same as those based on the non-Newtonian case and the Newtonian case. As the value of D_e decreases, the amplitude of the flexural waves becomes small. These are consistent with the curves of the dispersion and the attenuation.

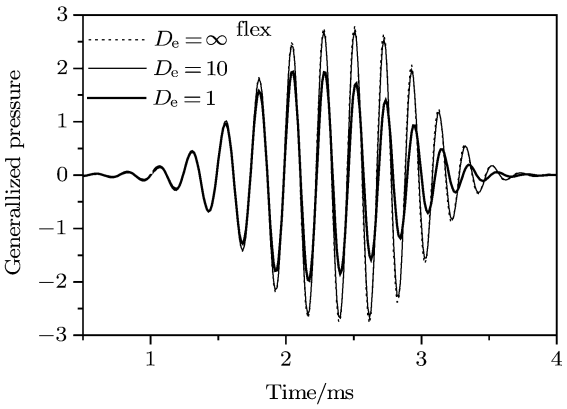


Fig. 5. Guided waveforms excited by a dipole source with 4-kHz source central frequency.

In Fig. 6 we plot the waveforms of the screw mode with 10-kHz source central frequency for three cases as Fig. 4. The arrival time of screw wave has a little change only in the deeply non-Newtonian, which is consistent with the curve of the dispersion. Moreover, as the value of D_e decreases, the amplitudes of the screw mode is obviously small, to which we should also pay attention even in the general non-Newtonian regime ($D_e = 10$). These results show that the non-Newtonian (Maxwell) fluid effect may be another factor of the acoustic guided wave attenuation.

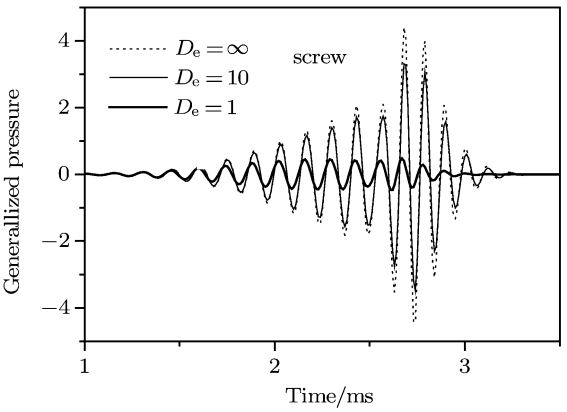


Fig. 6. Guided waveforms excited by a quadrupole source with 10-kHz source central frequency.

4. Conclusions

In the present paper, based on the generalized Biot–Tsiklauri model with a no-slip boundary, we investigated the influence of non-Newtonian effect on guided wave propagation of the fluid-filled borehole. We investigated the waveforms and the curves of velocity dispersion, and attenuation coefficients of the guided waves such as Stoneley waves, pseudo-Rayleigh waves, flexural waves, and screw waves due to a monopole, a dipole and a quadrupole source, respectively. The results show that non-Newtonian fluid effect in the saturated porous solid may be another important factor that influences acoustic guided waves in boreholes. In particular, the influence of non-Newtonian effect on attenuation of guided wave is obvious even in the general non-Newtonian regime ($D_{\mathrm{e}} = 10$). It is more significant to narrow down the discrepancy in attenuation between the theoretical prediction and the experimental measurement or field data. Although the velocity dispersion has a little change only in the deeply non-Newtonian regime, their changes are more distinct than those induced by the influence of squirt flow on fundamental guided waves.[21]

References

[1] Biot M A 1956 *J. Acoust. Soc. Am.* **28** 168
[2] Haire T J and Langton C M 1999 *Bone* **24** 291
[3] Hu H S 2003 *Acta Phys. Sin.* **52** 1951 (in Chinese)
[4] Guan W, Hu H S and Chu Z T 2006 *Acta Phys. Sin.* **55** 267 (in Chinese)
[5] Chen H, Wang X M and Zhao H B 2006 *Chin. Phys.* **15** 2819
[6] Zhang H L, Wang X M and Zhang B X 2004 *Acoustic Fields and Waves in Borehole* (Beijing: Science Press) (in Chinese)
[7] Rosenbaum J H 1974 *Geophysics* **39** 14
[8] Paillet F L and White J E 1982 *Geophysics* **47** 1215
[9] Norris A N 1989 *Geophysics* **54** 330
[10] Tang X M and Cheng C H 1996 *Geophysics* **61** 639
[11] Schmitt D P, Zhu Y and Cheng C H 1988 *J. Acoust. Soc. Am.* **84** 2230
[12] Zhang B X, Wang K X and Dong Q D 1995 *Chin. J. Geophysics* **38** (Suppl) 178 (in Chinese)
[13] Zhang B X, Wang K X and Dong Q D 1996 *J. Acoust. Soc. Am.* **99** 682
[14] Chang C, Nguyen Q D and Ronningsen H P 1999 *J. Non-Newtonian Fluid Mech.* **87** 127
[15] Tsiklauri D and I Beresnev 2001 *Phys. Rev.* E **63** 046304
[16] Tsiklauri D 2003 *Transport Porous Media* **53** 39
[17] Cui Z W, Liu J X and Wang K X 2003 *Waves Random Media* **13** 191
[18] Markov M G 2006 *Acoust. Phys.* **52** 429
[19] Kurkjian A L and Chang S K 1986 *Geophysics* **51** 148
[20] Cui Z W and Wang K X 2003 *Int. J. Eng. Sci.* **41** 2179
[21] Cui Z W, Liu J X and Wang K X 2005 *J. Jilin Univ.* (Natural Science Edition) **43** 803 (in Chinese)
[22] Yamamtoto T and Turgut A 1988 *J. Acoust. Soc. Am.* **83** 1744